

## Supplementary Information

### Title

The adhesion GPCR GPR116/ADGRF5 has a dual function in pancreatic islets  
regulating somatostatin release and islet development

### Authors

Juliane Röthe<sup>1</sup>, Robert Kraft<sup>2</sup>, Albert Ricken<sup>3</sup>, Isabell Kaczmarek<sup>1</sup>, Madlen Matz-  
Soja<sup>4,5</sup>, Karsten Winter<sup>3</sup>, André Nguyen Dietzsch<sup>1</sup>, Julia Buchold<sup>1</sup>, Marie-Gabrielle  
Ludwig<sup>6</sup>, Ines Liebscher<sup>1</sup>, Torsten Schöneberg<sup>1</sup>, and Doreen Thor<sup>1\*</sup>

### Affiliations

<sup>1</sup>Rudolf Schönheimer Institute of Biochemistry, Medical Faculty, Leipzig University,  
Leipzig, Germany

<sup>2</sup>Carl-Ludwig-Institute for Physiology, Medical Faculty, Leipzig University, Leipzig,  
Germany

<sup>3</sup>Institute of Anatomy, Medical Faculty, Leipzig University, Leipzig, Germany

<sup>4</sup>Medical Department II – Gastroenterology, Hepatology, Infectious Diseases,  
Pneumology, University Medical Center, Leipzig, Germany

<sup>5</sup>Division of Hepatology, Clinic and Polyclinic for Oncology, Gastroenterology,  
Hepatology, Infectious Diseases, and Pneumology, University Hospital, Leipzig,  
Germany

<sup>6</sup>Novartis Institutes for Biomedical Research, Basel, Switzerland

### Contact information

\*To whom correspondence should be addressed:

Doreen Thor, Telephone: +49 341 9722177

E-mail: doreen.thor@medizin.uni-leipzig.de

## 26 **Supplementary Results**

### 27 ***Stachel* peptide-mediated GPR116 activation**

28 Prior to the activation of endogenously expressed GPR116, we tested the specificity  
29 of p116 and p116sc in transfected cells (Supplementary Figs. 1c – g). GPR116 is  
30 activated by p116 resulting in a significant increase in the intracellular IP<sub>1</sub>  
31 concentration via activation of the G<sub>q/11</sub> protein/phospholipase C-signaling pathway,  
32 whereas the control peptide (p116sc) did not induce a response (Supplementary Fig.  
33 1c). In GPR116-transfected cells, the stimulation with p116 resulted in a 12-fold  
34 activation of NFAT reporter gene compared to mock-transfected cells whereas  
35 p116sc did not show any effect upon receptor activation (Supplementary Fig. 1d). In  
36 line with a phospholipase C-dependent mechanism, intracellular Ca<sup>2+</sup> transients were  
37 induced by p116 or by activation of endogenous purinergic receptors with ATP in  
38 GPR116-transfected HEK293T cells, while p116sc failed to evoke Ca<sup>2+</sup> signals.  
39 Mock-transfected cells did neither respond to p116 nor p116sc, whereas ATP  
40 strongly increased intracellular Ca<sup>2+</sup> levels (Supplementary Figs. 1e, f, and g). These  
41 data confirm that GPR116 signals via G<sub>αq/11</sub> protein/phospholipase C/Ca<sup>2+</sup> pathway  
42 upon stimulation with p116<sup>1-3</sup>.

### 43 **Characterization of GPR116 ko construct**

44 The constitutive GPR116 ko mouse strain was derived from exon-17-floxed mouse  
45 strain (*Gpr116<sup>fl/fl</sup>*)<sup>4</sup>. Exon 17 of *Gpr116* encodes for most of the 7-transmembrane  
46 helix domain mediating G-protein coupling. The same ko mouse line was used to  
47 study G-protein signaling of GPR116 in alveolar type II cells<sup>1</sup>. PCR analysis revealed  
48 *Gpr116* transcripts with exon 17 deletion ( $\Delta$ exon17-variant). The resulting open-  
49 reading frame encodes for a 7-TM-deficient receptor protein still containing the C-  
50 terminal half of the transmembrane helix 7 and the C terminus (Supplementary Figs.  
51 2a and 2b). *In vitro* expression of the  $\Delta$ exon17-variant in COS-7 cells showed a  
52 significantly reduced cell surface expression but unchanged total expression of  
53 truncated GPR116 compared to the full-length receptor (Supplementary Fig. 2c). This  
54 indicates intracellular retention of the receptor mutant but also an obvious portion of a  
55 plasma membrane-anchored N terminus of GPR116. However, IP<sub>1</sub> accumulation was  
56 completely abolished in cells expressing the mutant GPR116 indicating no functional  
57 G-protein coupling *in vitro* (Supplementary Fig. 2d).

## 58 **Supplementary Experimental Procedures**

### 59 **Cell culture and *in vitro* functional assays**

60 HEK293T and COS-7 cells were cultured in Dulbecco's minimum essential medium  
61 (DMEM) supplemented with 10 % fetal bovine serum (FBS), 100 units/ml penicillin,  
62 and 100 µg/ml streptomycin at 37 °C and 5 % CO<sub>2</sub> in a humidified atmosphere.

63 Generation of mouse GPR116 plasmid were described previously<sup>2</sup>.

64 Luciferase reporter gene assays and quantification of inositol 1 phosphate (IP<sub>1</sub>) were  
65 described previously<sup>2</sup>. Briefly, for luciferase reporter gene assays HEK293T cells  
66 were co-transfected with receptor plasmid (25 ng/well) and NFAT reporter construct  
67 (50 ng/well; PathDetect trans-reporting system) using Lipofectamine™ 2000  
68 according to the manufacturer's protocol. After 24 h HEK293T cells were treated with  
69 2 mM peptide solution or respective controls in phenol red-free DMEM for 5 h at  
70 37 °C. Stimulation was terminated by washing cells once with PBS and addition of  
71 100 µl luciferase assay reagent (SteadyLite, Perkin Elmer). The measurement of  
72 fluorescence intensity was performed with the EnVision Multilabel Reader (Perkin  
73 Elmer). Measurements of IP<sub>1</sub> were performed in COS-7 with the IP-One Tb kit  
74 (Cisbio) according to the manufacturer's protocol. Here, IP<sub>1</sub> accumulation is achieved  
75 by LiCl contained in the stimulation buffer which blocks the degradation of IP<sub>1</sub> to myo-  
76 inositol. 48 h after transfection COS-7 cells were incubated with IP<sub>1</sub> stimulation buffer  
77 containing 1 mM peptide or respective controls. After 30 min cells were lysed.  
78 Accumulated IP<sub>1</sub> was determined in cell extracts using ProxiPlate-384 Plus  
79 microplates (Perkin Elmer) with the EnVision Multilabel Reader (Perkin Elmer).

### 80 **Cell surface and total ELISA**

81 All receptor constructs carried an N-terminal HA and a C-terminal FLAG tag to permit  
82 for enzyme-linked immunosorbent assay (ELISA) -based receptor detection. Cell  
83 surface expression was analyzed using an indirect ELISA. Transiently transfected  
84 COS-7 cells were fixed with 4 % formaldehyde and incubated with blocking solution  
85 (media + 10 % FBS) for 1 h at 37 °C. ELISA was performed with an anti-HA-  
86 peroxidase-conjugated antibody (Roche) as previously described<sup>5</sup>.

87 A sandwich ELISA was used to estimate the total amounts of receptor constructs.  
88 After lysis of transfected COS-7 cells the total expression of receptors were analyzed  
89 with an anti-FLAG-M2- and an anti-HA-peroxidase-conjugated antibody (Roche) as  
90 previously described<sup>6</sup>.

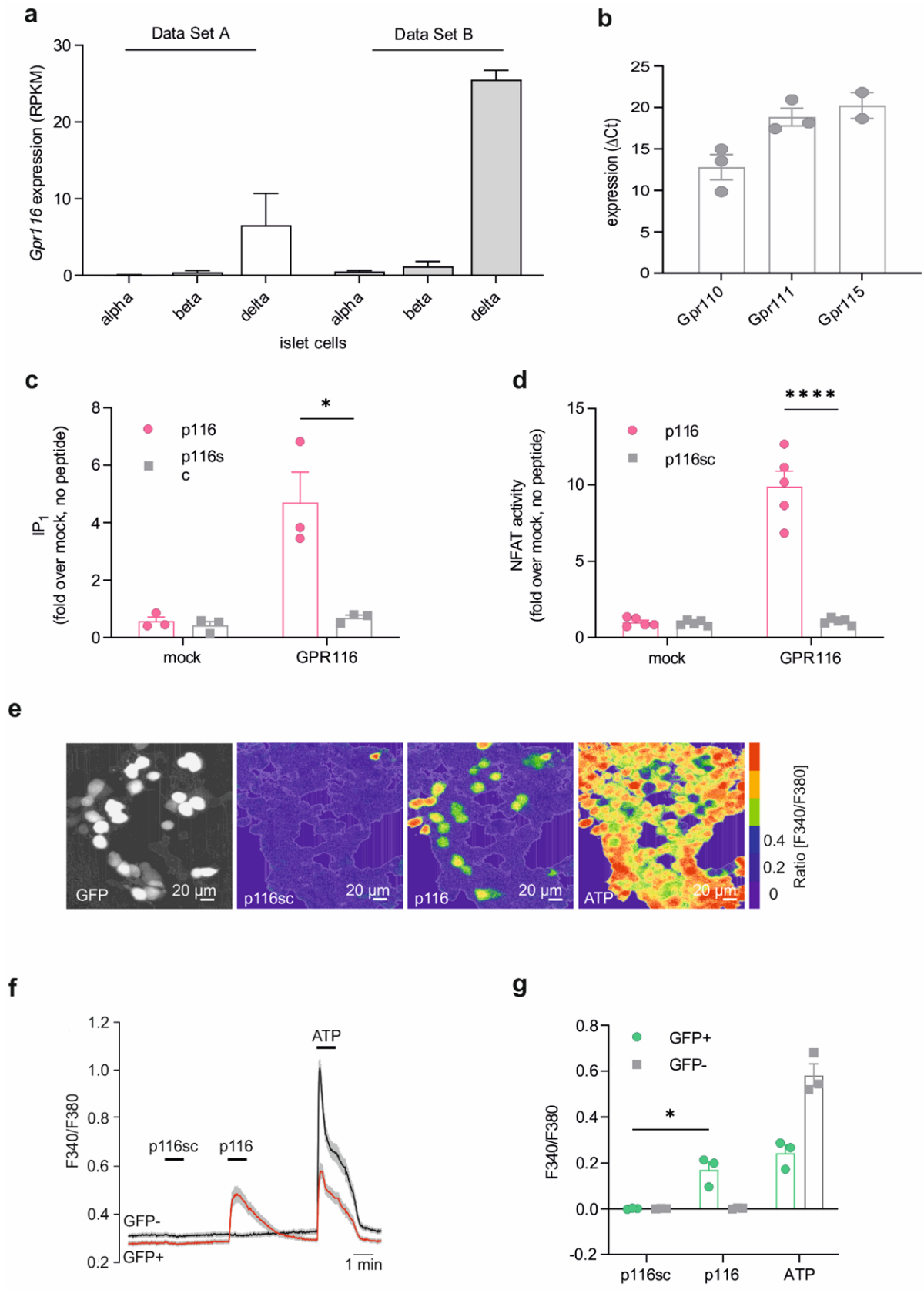
91 **Generation of GPR116 ko construct**

92 GPR116 ko construct was amplified from mouse lung cDNA with following primers:  
93 5'-ATCAGCATCCTTGACTTGCT (sense) and 5'-  
94 GCAGTAACTAGTCTACTTATCGTCGTCATCCTTGTAATCGTTGAGCAGTGAGTAA  
95 G (antisense). The reverse primer contained the FLAG-Tag and an *SpeI* restriction  
96 site. The PCR reaction was carried out with the Q5 polymerase (New England  
97 Biolabs) following the manufacturer's instructions. The reaction was initiated with a  
98 denaturation at 98 °C for 30 s, followed by 35 cycles of denaturation at 98 °C for  
99 10 s, annealing at 65 °C for 30 s and elongation at 72 °C for 60 s. The final  
100 amplification step was performed at 72 °C for 2 min. The PCR product was cut with  
101 *SpeI* and *EcoRI*, purified and ligated into the existing GPR116 plasmid (in the  
102 mammalian expression vector pcDps).

103 **Re-analysis of publicly available RNA-seq data sets**

104 Gene Expression Omnibus (GEO) database was searched for RNA-seq expression  
105 data of sorted pancreatic islets. Two different data sets (GSE760178 and (shown as  
106 Data Set A, GSE760178<sup>8</sup> and Data Set B, GSE806739<sup>9</sup>) indicate GSE806739) indicate  
107 <sup>8,9</sup> were evaluated regarding the expression of *Gpr116* in alpha-, beta-, and delta  
108 cells. The values are given in FPKM (Fragments Per Kilobase Million) or RPKM  
109 (Reads Per Kilobase Million) to normalize the expression for sequencing depth and  
110 gene length.

111 **Supplementary figures and tables**



112

113 **Supplementary Figure 1 –*Gpr116* expression in pancreatic islets and *Stachel***  
114 **peptide-mediated activation.**

115 (a) RNA-seq re-analyses of sorted pancreatic islets cells (shown as Data Set A,  
116 GSE76017<sup>8</sup> and Data Set B, GSE80673<sup>9</sup>) indicate that GPR116 is predominantly  
117 expressed in delta cells. Data are presented as mean of RPKM values  $\pm$  SD of two to  
118 six samples of each cell type.

119 (b) GPR116 belongs to a group of structurally related aGPCR, namely GPR110,  
120 GPR111, and GPR115. Since it has been shown that *Stachel*-derived peptides may  
121 activate related aGPCRs, we analyzed their expression in pancreatic islets. All three  
122 receptors are considerably less expressed compared to GPR116. Quantitative PCR  
123 data are presented as mean  $\pm$  SEM normalized to  $\beta$ -actin of at least two experiments  
124 performed in triplicates.

125 (c) IP<sub>1</sub> accumulation was measured after stimulation of GPR116- or mock-transfected  
126 COS-7 cells with the GPR116 agonist p116 (1 mM) or the inactive peptide p116sc  
127 (1 mM). Data are given as mean  $\pm$  SEM fold over non-stimulated mock-transfected  
128 cells (basal IP<sub>1</sub> level: 242.6  $\pm$  96.1 nM) of three independent experiments performed  
129 in triplicates.

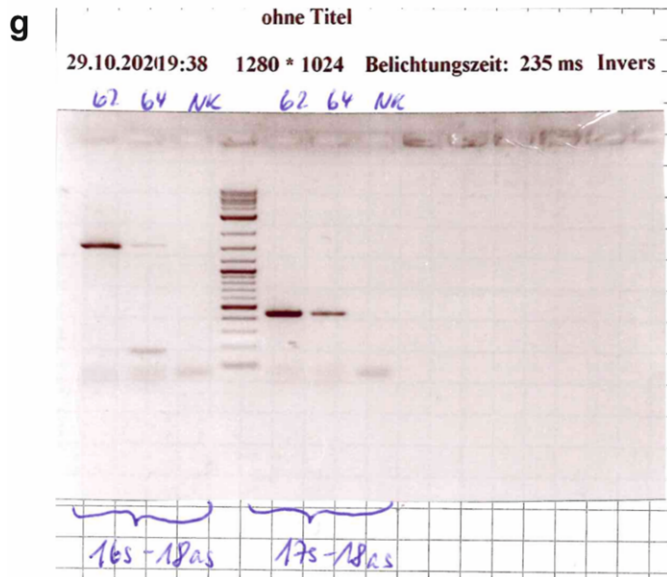
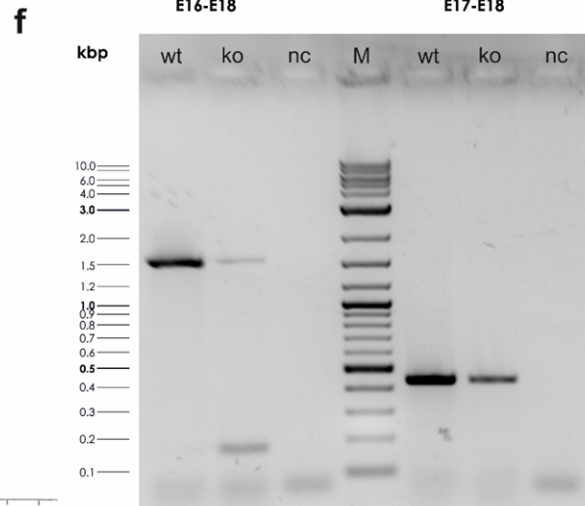
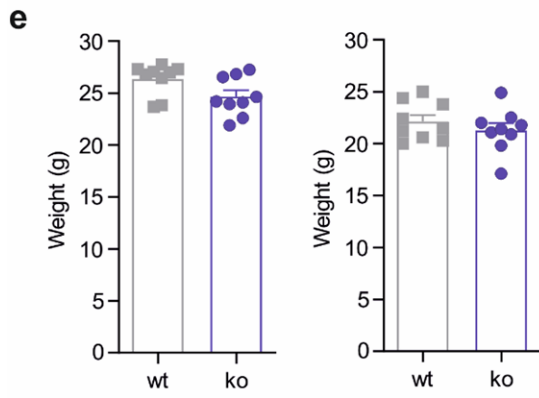
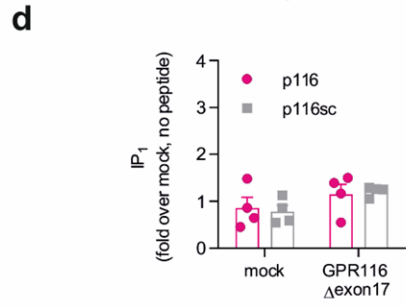
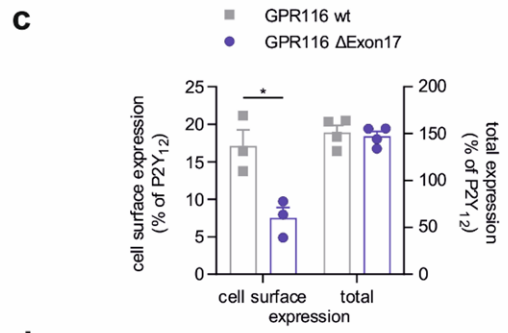
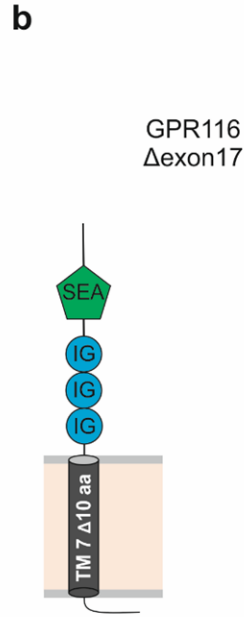
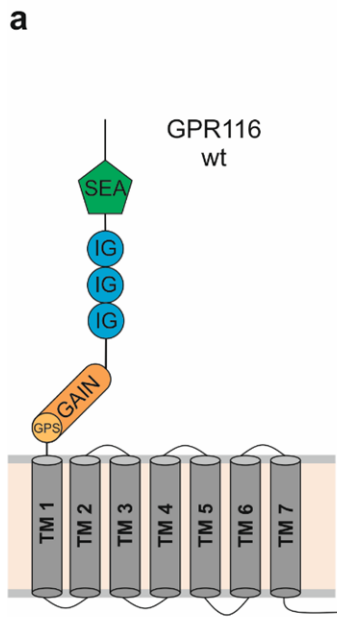
130 (d) NFAT-luciferase reporter gene assay indicates a gain of luciferase activity only in  
131 GPR116-transfected HEK293T cells after stimulation with 2 mM p116, whereas  
132 incubation with 2 mM p116sc does not change luciferase activity. Given is the  
133 mean  $\pm$  SEM as fold over non-stimulated mock-transfected cells (basal:  
134 889.7  $\pm$  409.5 counts) of n = 12 (p116) and n = 5 (p116sc) independent experiments  
135 performed in triplicates.

136 (e) Fura 2-based Ca<sup>2+</sup> imaging experiments were performed in HEK293T cells  
137 cotransfected with GPR116 and with GFP as transfection control. Representative  
138 images show the fluorescence ratio (F340/F380) after administration of p116sc  
139 (1 mM), p116 (1 mM), and ATP (100  $\mu$ M).

140 (f) Time course of Ca<sup>2+</sup> in GFP-positive (GFP+) and GFP-negative (GFP-) cells from  
141 the same coverslip, as shown in (c). Each trace represents the average Ca<sup>2+</sup>  
142 signal  $\pm$  SEM from 31 cells.

143 (g) Average Ca<sup>2+</sup> signals  $\pm$  SEM are presented as mean delta ratio  
144 (F340/F380)  $\pm$  SEM of three independent experiments each containing 25 to 49  
145 GFP+ and GFP- cells. Only GFP+ cells showed responses to p116 (1 mM). ATP

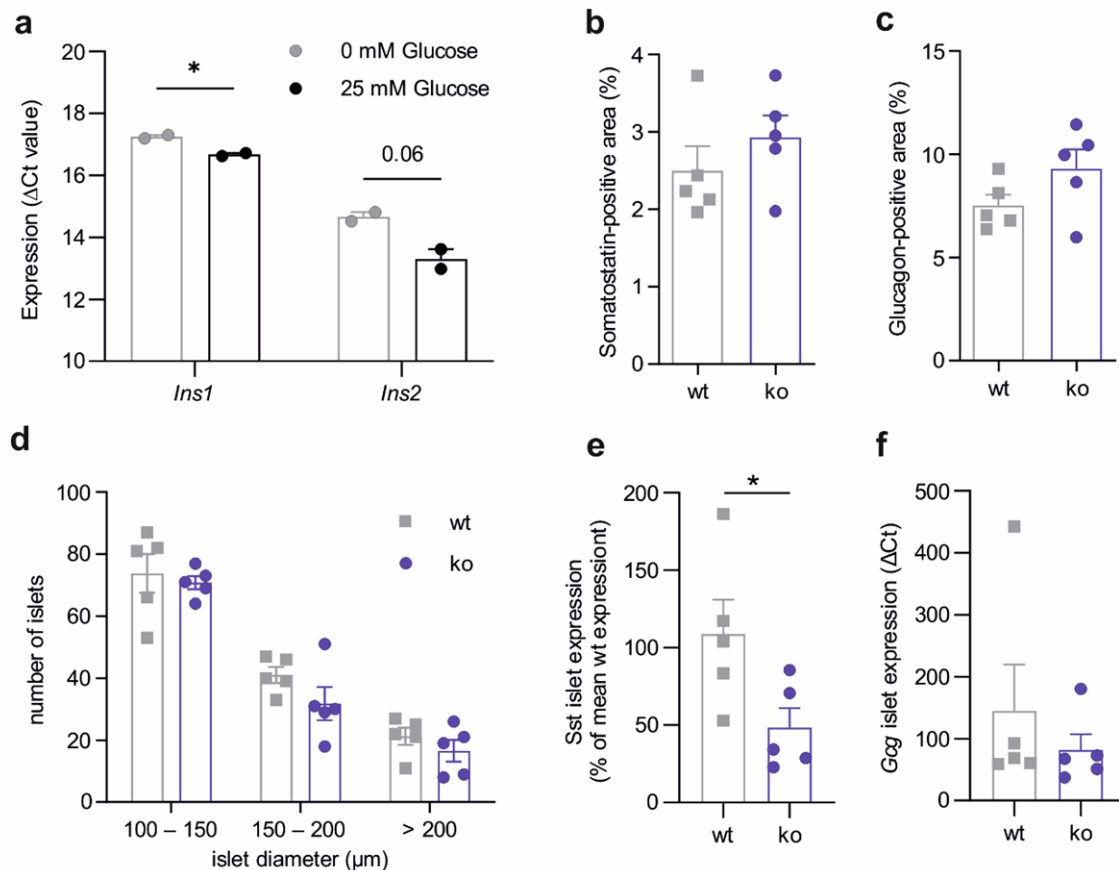
146 (100  $\mu$ M) induced signals in both GFP+ and GFP- cells, whereas p116sc was  
147 ineffective.  
148 P values were determined using an unpaired multiple t-test (Holm-Šídák method)  
149 (\*P  $\leq$  0.05, \*\*\*\*P  $\leq$  0.0001).



150



151 **Supplementary Figure 2 – Characterization of GPR116<sup>Δexon17</sup> construct.**  
152 (a & b) Schematic depiction of the GPR116 wt receptor and GPR116 ko receptor  
153 with deletion of exon 17.  
154 (c) Cell surface and total expression of mouse GPR116 wt and GPR116<sup>Δexon17</sup>  
155 receptor were detected in transfected COS-7 cells using an indirect or sandwich  
156 ELISA system, respectively. While total expression was unchanged, cell surface  
157 expression levels of GPR116<sup>Δexon17</sup> were decreased in comparison to the wt receptor,  
158 however, cell surface expression was still detectable. Values are given as  
159 percentage of P2Y<sub>12</sub> receptor as positive control (OE readings of P2Y<sub>12</sub>: 1.29 ± 0.13  
160 and 0.913 ± 0.034 for cell surface expression and total expression, respectively) and  
161 are shown as mean ± SEM for n = 3 (cell surface expression) and n = 4 (total  
162 expression) performed in triplicates. Non-specific OD values of empty vector  
163 transfected cells were 0.003 ± 0.001 (cell surface expression) and 0.064 ± 0.004  
164 (total expression).  
165 (d) IP<sub>1</sub> concentrations were quantified in mock- and GPR116<sup>Δexon17</sup>-transfected  
166 COS-7 cells after incubation with p116 (1 mM) and p116sc (1 mM). Data are shown  
167 as fold over non-stimulated mock-transfected cells (basal IP<sub>1</sub> level: 207.8 ± 76.1 nM)  
168 and given as mean ± SEM of four independent experiments performed in triplicates.  
169 (e) No differences in body weight of male (left panel) or female (right panel) between  
170 wt and ko mice were observed indicating that metabolic changes are not connected  
171 to an increase in body weight. Given is the mean ± SD of ten wt and ko mice.  
172 (f) PCR analysis of cDNA from pancreatic islets isolated from delta cell-specific  
173 *Gpr116* ko mice reveal partial deletion of *Gpr116*. Two different primer sets were  
174 used to amplify cDNA with sense primers located on exon 16 (lane 1 - 3) or exon 17  
175 (lane 5 - 7) and antisense primer located on exon 18. Given that exon 17 is deleted  
176 pancreatic delta cells due to Cre expression in somatostatin expressing cells, primer  
177 set E16/E18 should yield a smaller fragment, whereas primer set E17/E18 should  
178 have reduced amplification due to *Gpr116* expression in other islet cells. For  
179 reference, 1 kb Plus DNA Ladder (NEB) was used to identify the size of the PCR  
180 products. (g) Uncropped image of gel electrophoresis shown in (f).  
181



182

183 **Supplementary Figure 3 – Islet specific changes due to constitutive deficiency**  
 184 **of GPR116.**

185 (a) Isolated wt hepatocytes were incubated with different glucose concentrations (0  
 186 mM vs. 25 mM) for 24 hours and insulin expression was determined demonstrating  
 187 that increased glucose concentration stimulate expression of the insulin genes *Ins1*  
 188 and *Ins2*.

189 (b) The quantification of somatostatin-positive area is presented as ratio of  
 190 somatostatin-positive cells to total pancreatic islet area. Given is the mean  $\pm$  SEM of  
 191 five wt and ko mice.

192 (c) The quantification of glucagon-positive area is presented as ratio of glucagon-  
 193 positive cells to total pancreatic islet area. Given is the mean  $\pm$  SEM of five wt and ko  
 194 mice.

195 (d) Depending on islet diameter islets were grouped into small (<100  $\mu\text{m}$ ) (see  
 196 Fig. 5f), medium (100 – 150  $\mu\text{m}$ ), large (150 – 200  $\mu\text{m}$ ), and very large (>200  $\mu\text{m}$ )  
 197 islets. Islet numbers of each group were counted in all sections of five wt and ko  
 198 animals and are presented as mean  $\pm$  SD.

199 (e) Somatostatin expression (*SSt*) was determined in in adult islets from 5 wt and ko  
200 animals. Data is given as mean  $\pm$  SEM normalized to expression of  $\beta$ -actin as  
201 reference gene.

202 (f) Glucagon expression (*Gcg*) was determined in in adult islets from 5 wt and ko  
203 animals. Data is given as mean  $\pm$  SEM normalized to expression of  $\beta$ -actin as  
204 reference gene.

205 Statistical significance was tested using a two-tailed unpaired *t* test (\* $P \leq 0.05$ ).

206 **Supplementary Table 1: Primer sequences used for qPCR analyses in islets,**  
 207 **pancreas, liver, and cell lines.**

gene	Primer forward 5'-3'	Primer reverse 5'-3'
mouse <i>Gpr116</i>	GAACACGTCTTCTGCCCTCT	TGCCCTTGGTGAAGTGTGTC
mouse <i>Gpr110</i>	AGAGCAGGAGCTGAGAGCAG	ACGAGCCACAGAAGTCCAAT
mouse <i>Gpr111</i>	TGATCTGAAGGGAGACGACA	AGTACAACCAATGGGCAGGA
mouse <i>Gpr115</i>	GTGTGAAAAATGAAGCCCTG	CCTGTCTTGGTCTAAACTCA
mouse <i>Ins1</i>	GGGGAGCGTGGCTTCTTCTA	CCAAGGTCTGAAGGTCCCCG
mouse <i>Ins2</i>	TGACCTTCAGACCTTGGCACTG	GTAGAGGGAGCAGATGCTGGTG
mouse <i>Ide</i>	TGAAAAGGCTACGGGGAAC	ACGTCGATGCCTTCTTGTT
mouse <i>Pfkl Iso1</i>	TGAGGATGGCTGGGAGAACT	TGAACCACCAGATCCTTCACG
mouse <i>Pfkl Iso2</i>	CATTGACCGGCATGGAAAGC	TGCAGCCCTGGCTATTCAA
mouse <i>Ldha</i>	GTCCAGCGAAACGTGAACAT	TCCAAGCCACGTAGGTCAAG
mouse <i>Pklr</i>	CCGAGATACGCACTGGAGTC	GTGGTAGTCCACCCACACTG
mouse <i>Pygl</i>	CCTATGGCTACGGCATTCTGT	TCTCCAAGGGTTTCCATGC
mouse <i>Fbp1</i>	AGTCGTCCTACGCTACCTGT	TGGTTCCGATGGACACAAGG
mouse <i>Gys2</i>	TCACCGTTTTCTCTGAACCACT	CTGTTGGTCTGCATCAGGGT
mouse <i>Actb</i>	GCTCTTTTCCAGCCTTCCTT	CGGATGTCAACGTCACACTT
human GPR116	GAACACTTCCTCCGCCCTCT	TTCCAGACTTGAACCCTGTC
human ACTB	GCACTCTTCCAGCCTTCCTT	CGGATGTCCACGTCACACTT
rat <i>Gpr116</i>	GAACACATCCTCTGCCCTCT	TGCCCTTGGTGAAGTGTGTC
rat <i>Actb</i>	GCTCTCTTCCAGCCTTCCTT	CGGATGTCAACGTCACACTT

208

209 **Supplementary References**

- 210 1. Brown, K. *et al.* Epithelial Gpr116 regulates pulmonary alveolar homeostasis via  
211 Gq/11 signaling. *JCI insight* **2**, e93700; 10.1172/jci.insight.93700 (2017).
- 212 2. Demberg, L. M. *et al.* Activation of adhesion G protein-coupled receptors. Agonist  
213 specificity of *Stachel* sequence-derived peptides. *J. Biol. Chem.* **292**, 4383–4394;  
214 10.1074/jbc.M116.763656 (2017).
- 215 3. Tang, X. *et al.* GPR116, an adhesion G-protein-coupled receptor, promotes breast  
216 cancer metastasis via the Gαq-p63RhoGEF-Rho GTPase pathway. *Cancer Res.*  
217 **73**, 6206–6218; 10.1158/0008-5472.CAN-13-1049 (2013).
- 218 4. Bridges, J. P. *et al.* Orphan G protein-coupled receptor GPR116 regulates  
219 pulmonary surfactant pool size. *Am. J. Respir. Cell Mol. Biol.* **49**, 348–357;  
220 10.1165/rcmb.2012-0439OC (2013).
- 221 5. Stäubert, C., Broom, O. J. & Nordström, A. Hydroxycarboxylic acid receptors are  
222 essential for breast cancer cells to control their lipid/fatty acid metabolism.  
223 *Oncotarget* **6**, 19706–19720; 10.18632/oncotarget.3565 (2015).
- 224 6. Römpler, H., Yu, H.-T., Arnold, A., Orth, A. & Schöneberg, T. Functional  
225 consequences of naturally occurring DRY motif variants in the mammalian  
226 chemoattractant receptor GPR33. *Genomics* **87**, 724–732;  
227 10.1016/j.ygeno.2006.02.009 (2006).
- 228 7. Hara, M. *et al.* Transgenic mice with green fluorescent protein-labeled pancreatic  
229 beta -cells. *American journal of physiology. Endocrinology and metabolism* **284**,  
230 E177-83; 10.1152/ajpendo.00321.2002 (2003).
- 231 8. Adriaenssens, A. E. *et al.* Transcriptomic profiling of pancreatic alpha, beta and  
232 delta cell populations identifies delta cells as a principal target for ghrelin in mouse  
233 islets. *Diabetologia* **59**, 2156–2165; 10.1007/s00125-016-4033-1 (2016).
- 234 9. DiGruccio, M. R. *et al.* Comprehensive alpha, beta and delta cell transcriptomes  
235 reveal that ghrelin selectively activates delta cells and promotes somatostatin  
236 release from pancreatic islets. *Molecular metabolism* **5**, 449–458;  
237 10.1016/j.molmet.2016.04.007 (2016).